Andrzej Wójtowicz, Patrycja Janiak, Santina Topolska

Testing the Quality of Welded Joints in Thick-Walled Pipes Used in the Power Industry

Abstract: The article discusses tests concerning the quality of joints in relation to the service life of thick-walled pipes made of steel P355NH using the TIG welding method (141) and filler metal alloy grade SNi6625 (Inconel 625). Because of its mechanical properties, corrosion resistance and high-temperature resistance, the above-named material is commonly used in various industries. The test joints were subjected to structural, non-destructive and corrosion resistance-related tests.

Keywords: steel P355NH, non-destructive tests, neutral salt spray-based corrosion resistance tests, microstructure, hardness tests, filler metal SNi6625

DOI: *10.17729/ebis.2022.3/2*

Introduction

The power sector today is continuously searching for more precisely selected and specialised engineering materials able to satisfy technological requirements arising from the complexity of various processes. Power systems should be reliable, failure-free and characterised by operational safety. One of the factors impeding the satisfaction of the above-named needs is the fact that most elements are exposed to high internal pressure and, as a result, are subject to the Pressure Equipment Directive.

This article contains recommendations related to the use of specific materials, which, in accordance with related guidelines, are characterised by parameters preventing, among other things, the phenomenon of brittle cracking, potentially posing a significant operation-related threat [1, 2].

Factors affecting the service life of (and posing a threat to) elements and components used in the power industry include high temperature, corrosion processes as well as both surface and volume-related material discontinuities. Each joint in the system must be characterised by appropriate quality guaranteeing the safe and continuous operation of a given unit. For this reason, particular attention should be paid to the adjustment and control of parameters being of key importance as regards the proper course of technological processes. Non-destructive tests are indispensable in quality assessment as they do not affect material integrity when identifying the presence of potential imperfections [3].

The material, which, because of its availability and affordability, has become very competitive as capable of satisfying structural and

inż. Andrzej Wójtowicz – Łukasiewicz Research Network – Instytut Spawalnictwa, Research Group for Non-Destructive Tests ; inż. Patrycja Janiak; dr hab. inż. Santina Topolska – Silesian University of Technology, Faculty of Mechanical Engineering, Department of Welding

technological requirements of power sector equipment is unalloyed steel. Unalloyed steels are usually low-carbon steels after normalising, characterised by the ferritic-pearlitic structure. A steel grade frequently used in the power sector is P355NH. Steels used to make welded joints in power generation systems should be characterised by the fine-grained structure, good weldability and usability at a nominal temperature of approximately 400°C [4–6].

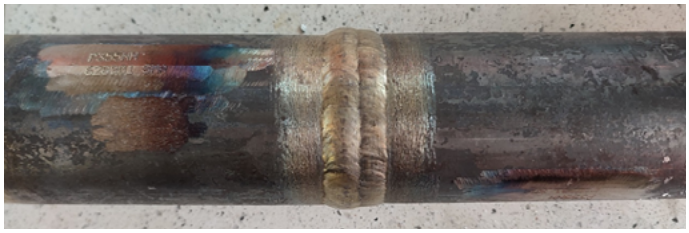

Fig. 1. Test specimen

Materials and tests

The tests involved a fragment of a tubular element made of steel P355NH (Fiug.1), whose favourable weldability and fined-grained structure enable its operation in accordance with the Pressure Equipment Directive and related standards. Welding processes utilising arc burning between a non-consumable tungsten electrode and a work piece (material being welded) are well-established as regards the joining of tubes. Having the aforesaid aspect in mind, the test joint was made using the TIG method (141), where the shielding (inert) gas was argon having a purity of 99.998%. The fact that the base material lacked corrosion resistance necessitated the use of the filler metal, i.e. alloy SNi6625 (NiCr22Mo9Nb), the popularity of which in the welding sector results directly from its mechanical properties, high-temperature wear resistance and very high corrosion resistance in aggressive environments. Detailed information concerning welding process parameters is contained in Table 1. The material parameters and the primary mechanical properties of alloy Inconel 625 (NiCr22Mo9Nb) are presented in Tables 4 and 5 [9, 10].

Table 1. Welding process parameters in accordance with preliminary welding procedure specification (pWPS)

Base material/dimensions	P355NH ϕ57.0 x 12.5 mm
Filler metal/dimensions	SNi6625 (NiCr22Mo9Nb) 2.0 mm – 2.4 mm
Method	TIG (141)
Current [A]	100-140
Voltage [V]	12-14
Electrode type	WT20
Heat input [kJ/mm]	0.8-1.5
Interpass temperature [˚C]	<150
Shielding gas	Ar 4.8 99.99%
Shielding gas flow rate [l/min]	7-13
Type of weld	butt weld
Welding position	inclined position (pipe fixed), rising welding (H-L045)

Table 2. Chemical composition of steel P355NH [7]

Grade	**Chemical element content1) [% by weight]**					
	C	Mn	Si	Mo	V	Nb
P355NH	≤0.20	0.90-1.70	max 0.50	max 0.08	≤0.10	≤0.05

Table 3. Primary mechanical properties of steel P355NH [8]

Grade	**Minimum mechanical properties**			
	R_m [MPa]	R_{eH} ($R_{p0.2}$) [MPa]	A [%]	KV [J]
				-20°C
P355NH	490	355	22	40

Tests

The investigation concerning the quality of the girth-welded joint involved the performance of both non-destructive and destructive tests.

The test joint was subjected to the Vickers microhardness test aimed to identify the resistance of the joint to local forces affecting it in the point-like manner. Subsequent tests involved the assessment of the microstructure

Table 4. Chemical composition of alloy NiCr22Mo9Nb [8, 9]

Grade	Chemical element content [% by weight]								
	C	Si	Mn	Ni	Cr	Mo	Nb	Fe	Ti
NiCr22Mo9Nb	≤0.1	≤0.5	≤0.5	≤58	20-23	8-10	3.15-4.15	≤5	≤0.5

Table 5. Primary mechanical properties of alloy NiCr22Mo9Nb [8, 9]

Grade	Minimum mechanical properties						
	R_m [MPa]	$R_{eH}(R_{p0.2})$ [MPa]	A [%]	E [GPa]	KV [J]		Maximum operating temperature, [°C]
					+20°C	-196°C	
NiCr22Mo9Nb	800	540	38	200	200	160	1000

of the base material, heat affected zone (HAZ) and that of the weld. The test specimens were obtained by cutting across the test tube entirely. The cutting process was performed using a semi-automatic saw involving the use of water and synthetic coolant-based cooling agents. After cutting, the test specimens were subjected to grinding performed in order to obtain required surface roughness. The final specimen preparation phase included polishing.

Vickers microhardness tests

The Vickers microhardness tests were performed using a Micromet 5013 hardness tester and a pyramidal diamond indenter (angle between opposite walls being 136°). The tests were performed along 3 parallel measurement lines. Line 1 and 2 contained 15 equidistant measurement points, whereas line 3 contained 12 such points. Each point was affected by an indenter load of 0.98 N for 15 seconds. Figure 2 presents the schematic arrangement of the measurement points in the key areas of the welded joint.

Microscopic tests

To reveal the microstructure of the test joint it was necessary to perform the etching of its surface. Due to the necessity of using various methods and etchants in different areas of the joint, the etching process consisted of two stages. The first stage was concerned with the base material and aimed to reveal the structure of the heat affected zone. The HAZ was subjected to etching with Adler's reagent II for 20 seconds. The second stage aimed to reveal the weld structure. The 20 second-long etching process was performed using the electrolytic anodic technique and a DC voltage of 2 V. The etchant used in the process was the solution of chromium oxide (VI) and sulphuric acid (VI).

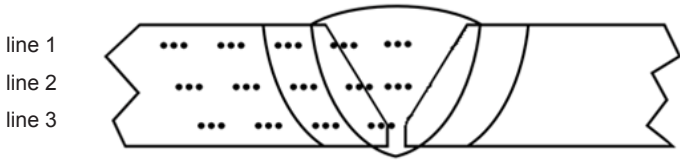

Fig. 2. Schematic arrangement of measurements points in the cross-section of the joint

Non-destructive tests

The first non-destructive test was the visual test, the performance of which is obligatory in cases of special processes (e.g. welding). The procedure was consistent with the instructions specified in the PN EN ISO 13018 standard (concerning VT-related general principles) and the PN EN ISO 17637 standard (describing visual tests of welded joints). The visual inspection-related technique involved direct local observation. All the observation conditions connected with the application of the above-named technique were met. The assessment of the test results was performed in accordance with the PN EN ISO 5817 standard.

The second non-destructive test was the wet dye penetrant test performed in accordance with the guidelines and under observation conditions consistent with the PN EN ISO 3059 and PN EN ISO 3452-1 standards. The above-named

standards are concerned with PT-related observation conditions and general principles. The test results were assessed in accordance with the PN EN ISO 23277 standard.

The final non-destructive test was the magnetic particle test, whose observation-related conditions and general principles are very similar to those concerning the penetrant test. The magnetic particle tests were performed in accordance with the requirements specified in the PN EN ISO 3059 and PN EN ISO 17638 standards. The test, involving stream magnetisation and the use of a rigid coil, was based on the wet fluorescent method. The test results were assessed in accordance with the criteria specified in the PN EN ISO 23278 standard.

The acceptance criterion applying to all of the above-presented tests was quality level B. As regards visual tests (VT), the PN EN ISO 5817 standard applies directly to quality level B. However, in cases of penetrant and magnetic particle tests it was necessary to apply the correlating PN EN ISO 17635 standard, where quality level B is identical to acceptance level 2X in accordance with the PN EN ISO 23277 and PN EN ISO 23278 standards in the penetrant and magnetic particle tests respectively.

All the penetrants were checked before the tests. All of the measurement devices were fully operational after a certified metrological inspection [10–18].

Corrosion tests

The corrosion tests, performed in a salt spray chamber, aimed to determine the corrosion resistance in a neutral salt spray environment. The salt spray chamber enables the "simulation" of exposure to an adverse environment for between several and twenty years. The above-named tests aimed to exclude the possible presence of surface discontinuities (if any), which could speed up the corrosion-triggered damage to the steel.

The neutral salt spray test (NSS) test was performed in accordance with the PN EN ISO 9227 and PN EN ISO 16701 standards. The tests involved the application of a CC450XP cyclic corrosion test chamber (Ascott) and a 5% solution of sodium chloride (with distilled water used as the solvent). The test parameters, consistent with the requirements specified in the above-named standard, are presented in Table 6. All the parameter values were restricted within ranges specified in the aforesaid standards. The test specimens were exposed to the effect of salt spray for 168 hours. After the test, the corrosion products were removed from the specimen, whereas the specimen itself was subjected to drying and weighing (aimed to identify the change of the specimen weight). The subsequent stage involved the calculation of the corrosion rate, where the active area of a given element was determined using the CAD software programme (applied in order to model the precise shape of the weld) [19, 20].

Table 6. Corrosion environment parameters [19]

	Measured values	**Proper values in accordance with PN EN ISO 9227**
Conductivity [µS/cm]	4	max 20
Density [g/cm^3]	1.032	between 1.029 and 1.036
pH	6.8	between 6.4 and 7.2

Test results and analysis

Vickers microhardness test results

The values obtained in a total of 75 measurements are presented in the hardness distribution diagram below (Fig. 3). In terms of the base material, the average value amounted to 188 HV0.1 in relation to three measurements lines. The steel was characterised by hardness typical of this grade (after annealing), i.e. approximately 175 HV0.1. It was possible to observe an increase in the base material hardness up to 200 HV0.1. In turn, the hardness of the weld increased up to 310 HV0.1. Both of the above-presented values indicated the proper

performance of the welding process. The average hardness of the weld amounted to 267 HV0.1. The aforesaid value did not exceed the difference between the hardness of the base material and that of the weld amounting to 100 HV0.1 (being the criterion of good weldability).

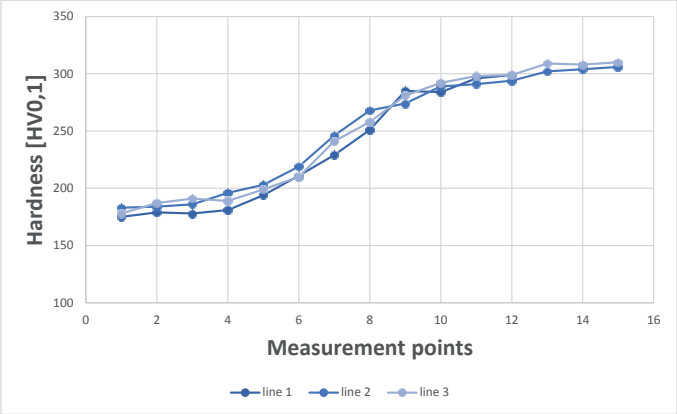

Fig. 3. Microhardness distribution in the cross-section of the welded joint

Microstructural test results

The assessment of the welded joint, presented in Figures 4 through 11, revealed that its microstructure indicated the proper performance of the welding process. The base material, visible in Figure 4 was characterised by the ferritic-pearlitic structure of banded nature. During the welding process, the base material was exposed to high temperature, which resulted in the formation of specific areas of the heat affected zone (HAZ), varying in the grain size (see Figures 5, 6 and 7). The HAZ area adjacent to the base material and farthest from the heat source contained traces of annealing within temperature ranges A1 and A3. The crystallisation process affected the areas characterised by the lowest transformation temperature, i.e. pearlite (Fig. 5). The areas closer to the fusion line were (along with progressing normalisation) characterised by the decreased grain size of the equiaxial ferritic-pearlitic structure. The area near the fusion line contained the ferritic-bainitic structure with visible boundaries of former austenite grains (Fig. 6). The austenite grains were characterised by a sharp growth resulting from high temperature affecting this area of the joint. The cooling process was accompanied by the formation of the coarse-grained structure, adjacent to the fusion line of alloy SNi6625 (Fig.

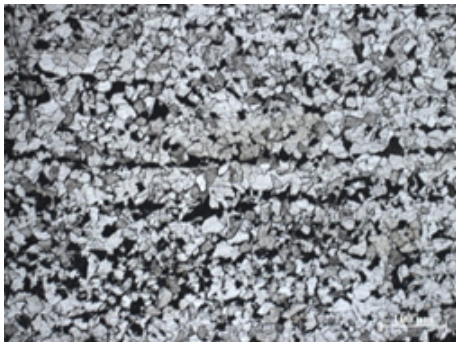

Fig. 4. Base material; mag. 200x

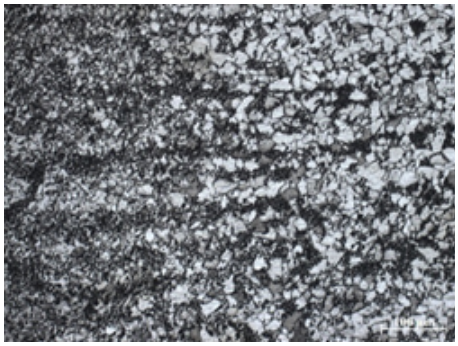

Fig. 5. Heat affected zone and the base material, the area of partial normalisation; mag. 200x

Fig. 6. Heat affected zone, normalisation area; mag. 200x

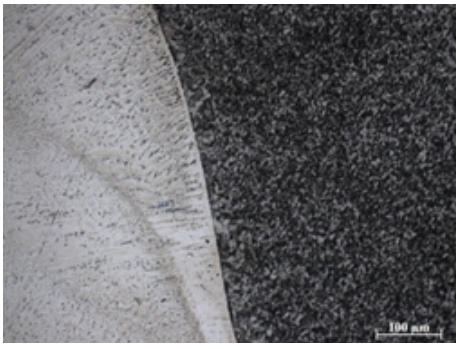

Fig. 7. Weld with the fusion line; mag. 200x

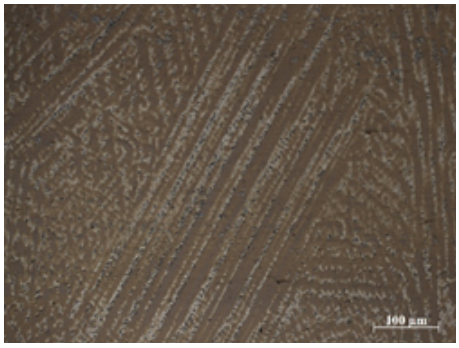

Fig. 8. Weld; mag. 200x

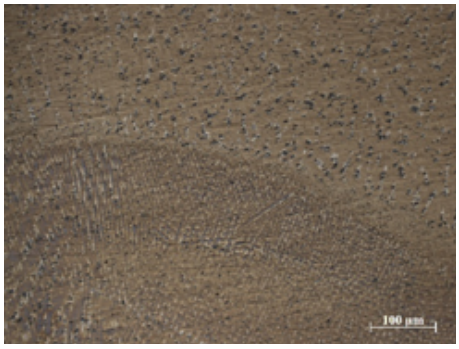

Fig. 9. Weld; mag. 200x

7). The weld structure was consistent with characteristics discussed in related publications concerning alloy Inconel 625. Figures 8–11 present columnar-dendritic structures, characteristic of welds made of high-alloy steels and nicker alloys. It is also possible to observe the multi-run nature of the weld.

Fig. 10. Weld; mag. 200x

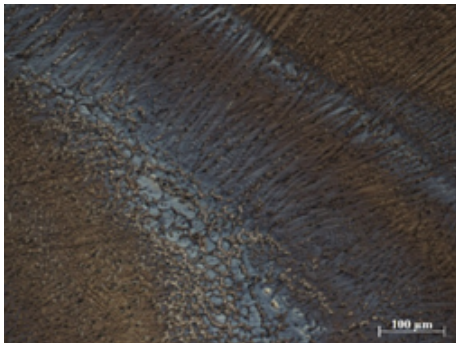

Fig. 11. Weld; mag. 200x

Non-destructive test results

The visual test-based assessment of the joint did not reveal the presence of imperfections making the joint inconsistent with the acceptance criteria related to quality level B. The weld was characterised by the proper shape and geometrical dimensions. Individual beads were made carefully and uniformly. The penetrant test, whose stages are presented in Figures 12 and 13, did not reveal the presence of any indication failing to satisfy the requirements of quality level 2X. The time of penetration and development amounted to 15 minutes. Before the test, penetrants and developers (H.Klumpf) were checked using reference specimen no. 2. In spite of using a more precise technique (i.e. wet fluorescent method), the magnetic particle test did not reveal the presence of any indications either. The test was performed using a test rig composed of a rigid coil and a UV-A light source (Figures 14 and 15). To ensure the recognition of the test as

Fig. 12. Specimen with the penetrant applied

Fig. 13. Specimen with the developer applied

Fig. 14. Magnetic particle test rig – rigid coil

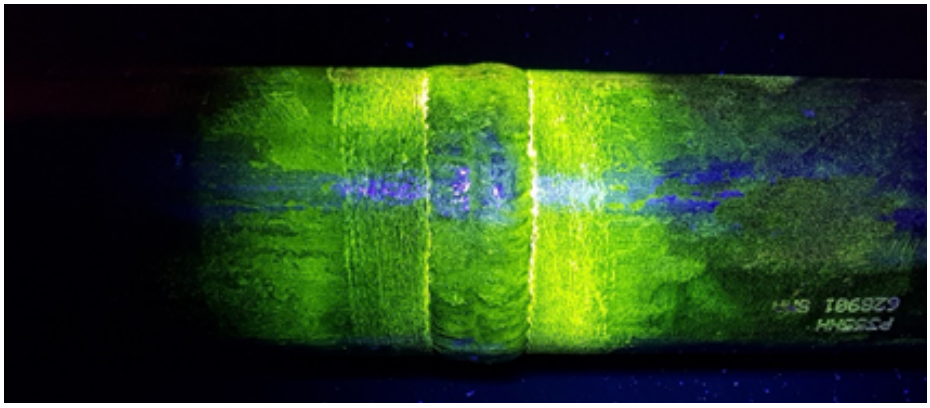

Fig. 15. Specimen after the magnetic particle test

performed properly, the value of illuminance should not exceed 20lx.

All of the tests confirmed the previously assumed acceptance criterion, i.e. quality level B, which, in relation to penetrant and magnetic particle tests (PT and MT) corresponds to acceptance level 2X.

Fig. 16. Specimen after 48 hours' exposure in the salt spray chamber

Fig. 17. Specimen after 168 hours' exposure in the salt spray chamber

Fig. 18. Face of the specimen after 168 hours' exposure in the salt spray chamber

Fig. 19. Specimen of the corrosion resistance test with the corrosion products removed

Corrosion resistance test results

The test results concerning resistance to the effect of neutral salt spray were observed after 48 hours and 168 hours. The observation was performed by the unaided eye. Already the first test revealed that the specimen underwent significant damage. However, it should be noted that, in terms of corrosion progression, the weld material significantly differed from that of the base material (Fig. 16). After 168 hours, the corrosion process was significantly more advanced; the tarnish of the weld was considerably greater than that observed after 48 hours. Figures 17 and 18 present the specimen before, whereas Figure 19 presents the specimen after the removal of the corrosion products. The weld surface compared with Figure 1, i.e. presenting the specimen before the corrosion test, was more tarnished, which could imply that also the weld underwent corrosion (to a slight extent).

Table 7 presents parameters necessary for calculating the linear rate of corrosion and mass decrement.

The information contained in the PN-H-04610:1978 and PN-H-04608:1978 standards as well as formulas 1, 2 and 3 were used to perform calculations concerning mass and linear mass decrements. The results of the calculations are presented in Table 8, along with the attribution of appropriate levels of corrosion resistance [21,22].

$$V_c = \frac{|\Delta m|}{A \cdot t} \quad (1)$$

$$V_p = V_c \cdot \alpha \quad (2)$$

$$\alpha = \frac{365}{1000 \cdot d} \quad (3)$$

Table 7. Information necessary for corrosion-related calculations

Specimen active area, A, [10^{-6} m^2]	Initial mass [g]	Mass after the test [g]	Difference in mass $\|\Delta m\|$ [g]	Time of exposure [h]
68811.887	3188.5	3180	8.5	168

where V_c – mass decrement/growth [g/m² × 24 hours], $|\Delta m|$ – difference in the mass of the specimens [g], A – area of the specimen subjected to corrosion [m²], t – time of specimen exposure in the salt spray chamber [24 hours], V_p – linear rate of corrosion [mm/year], d – density of the material subjected to corrosion [g/cm³], α – coefficient linking specimen mass decrement to the linear rate of corrosion.

Table 8. Corrosion resistance calculation results

Mass decrement, V_c [g/m² × 24 hours]	17.6465
Coefficient linking specimen mass decrement to the linear rate of corrosion, α	0.0465
Rate of corrosion, V_p [mm/year]	0.8206
Level of corrosion resistance, ^{0}k	7

Summary and conclusions

The performance of a total of 75 point microhardness measurements across the entire cross-section of the welded joint enabled the reliable assessment of the results obtained in the tests. It was possible to observe a significant increase in the weld hardness in comparison with that of the base material, which indicated the proper performance of the welding process. Both in terms of steel P355NH and alloy Inconel 625, the measurement values did not differ from those presented in related publications.

The microscopic observation of the base material confirmed the presence of the expected (and visibly banded) ferritic-pearlitic structure. The individual areas of the heat affected zone (HAZ) contained the microstructure typical of the TIG welding process. The weld area contained columnar-dendritic groups characterised by significant interdendritic segregation. The above-named microstructural morphology is characteristic of solidified welds made of high-alloy steels and nicker alloys. The weld properly penetrated the base material. The non-destructive tests did not reveal the presence of any surface discontinuity which could affect the service life of the joint (and potentially speed up corrosion processes). The adopted acceptance criterion was satisfied.

The corrosion resistance tests, performed in the atmosphere of neutral salt spray for 168 hours, revealed that the base material (BM) was significantly damaged, whereas the weld was considerably less damaged (than BM). The aforesaid process was also manifested by the change of the weld surface. After the test, the initially glossy weld surface was tarnished (mat). The removal of the corrosion products from the specimen revealed the presence of clearly visible corrosion pits in the base material.

In view of the above-presented observations it could be stated that both the selection of the filler metal and the performance of the welding process were appropriate. It was possible to demonstrate both the obtainment of the required quality in relation to the welded joint made of thick-walled tubes and the satisfaction of acceptance criteria specified for the power industry.

References

[1] Adamiec J.: High temperature corrosion of power boiler components cladded with nickel alloys, Materials Characterization, 2009, no. 60, pp. 1093–1099.
[2] Dyrektywa 97/23/WE Parlamentu Europejskiego i Rady z dnia 29 maja 1997 r. w sprawie zbliżenia ustawodawstw Państw Członkowskich dotyczących urządzeń ciśnieniowych (Dz. Urz. WE No. L 181).
[3] Rachwał A., Wolniak R.: Niezgodności spawalnicze i techniki ich wykrywania, Zeszyty Naukowe Politechniki Śląskiej, seria: Organizacja i zarządzanie, z. 117, Gliwice 2018.
[4] Dobrzański L.A.: Podstawy nauki o materiałach i metaloznawstwo, Wydawnictwa Naukowo-Techniczne, Warszawa 2002, pp. 617–620.
[5] Cieslak M.: The welding and solidification metallurgy of alloy 625, Welding Research Supplement, pp. 49–56.
[6] Petrzak P., Kowalski K., Rozmus-Górnikowska M.: Mikrostruktura i

skład chemiczny powłok ze stopów Inconel 625 i 686 napawanych metodą CMT na stali 16Mo3, Przegląd Spawalnictwa, vol. 89, no. 6, pp. 24–29.
[7] Polski Komitet Normalizacyjny, Norma PN-EN 10216-3:2014 Rury stalowe do zastosowań ciśnieniowych. Warunki techniczne dostawy. Część 3: Rury ze stali stopowych drobnoziarnistych.
[8] Polski Komitet Normalizacyjny, Norma PN-EN 10273:2016-09 Pręty walcowane na gorąco ze stali spawalnych o określonych własnościach w podwyższonych temperaturach na urządzenia ciśnieniowe.
[9] Polski Komitet Normalizacyjny, Norma PNE-EN ISO 18274:2011 Materiały dodatkowe do spawania – Druty i taśmy elektrodowe, druty i pręty do spawania niklu i stopów niklu – Klasyfikacja.
[10] Polski Komitet Normalizacyjny, Norma PN EN ISO 5817:2014, Spawanie – Złącza spawane ze stali, niklu, tytanu i ich stopów (z wyjątkiem spawanych wiązką) – Poziomy jakości według niezgodności spawalniczych.
[11] Polski Komitet Normalizacyjny, Norma PN EN ISO 23277:2015, Badania nieniszczące spoin – Badania penetracyjne – Poziomy akceptacji.
[12] Polski Komitet Normalizacyjny, Norma PN EN ISO 23278:2015, Badania nieniszczące spoin – Badania magnetyczno-proszkowe – Poziomy akceptacji.
[13] Polski Komitet Normalizacyjny, PN EN ISO 17635:2017, Badania nieniszczące spoin – Zasady ogólne dotyczące metali.
[14] Polski Komitet Normalizacyjny, PN EN ISO 17637:2017, Badania nieniszczące złączy spawanych – Badania wizualne złączy spawanych.
[15] Polski Komitet Normalizacyjny, PN EN ISO 17638:2017, Badanie nieniszczące spoin – Badanie magnetyczno-proszkowe.
[16] Polski Komitet Normalizacyjny, PN EN ISO 13018:2016, Badania nieniszczące – Badania wizualne – Zasady ogólne.
[17] Polski Komitet Normalizacyjny, PN EN ISO 3452-1:2021, Badania nieniszczące – Badania penetracyjne – Część 1: Zasady ogólne.
[18] Polski Komitet Normalizacyjny, PN EN ISO 3059:2013, Badania nieniszczące – Badania penetracyjne i badania magnetyczno-proszkowe – Warunki obserwacji.
[19] Polski Komitet Normalizacyjny, Norma PN-EN ISO 9227:2017, Badania korozyjne w sztucznych atmosferach – Badania w rozpylonej solance.
[20] Polski Komitet Normalizacyjny, Norma PN-EN ISO 16701:2015, Korozja metali i stopów – Korozja w sztucznych atmosferach.
[21] Polski Komitet Normalizacyjny, Norma PN-H-04610:1978, Korozja metali – Metody oceny badań korozyjnych (norma wycofana, brak zastąpienia).
[22] Polski Komitet Normalizacyjny, Norma PN-H-04608;1978, Korozja metali – Skala odporności metali na korozję (norma wycofana, brak zastąpienia).